

Pressure driven magnetic phase change in $\text{CrI}_3/\text{Br}_3\text{Cr}_2\text{I}_3$ heterostructure

Electronic Supplementary Information

Fazle Subhan¹, Luqman Ali², Razia Aman³, Yanguang Zhou^{*4}, Zhenzhen Qin^{*5}, and Guangzhao Qin^{*1,6,7}

1. *State Key Laboratory of Advanced Design and Manufacturing Technology for Vehicle, College of Mechanical and Vehicle Engineering, Hunan University, Changsha 410082, P. R. China*
2. *Department of Pharmacology, University of Virginia, 22903, Charlottesville, VA, USA*
3. *Department of Chemical Sciences, University of Lakki Marwat, Lakki Marwat 28420, KPK, Pakistan*
4. *Department of Mechanical and Aerospace Engineering, The Hong Kong University of Science and Technology, Clear Water Bay, Kowloon, Hong Kong SAR*
5. *International Laboratory for Quantum Functional Materials of Henan, and School of Physics and Microelectronics, Zhengzhou University, Zhengzhou 450001, P. R. China*
6. *Research Institute of Hunan University in Chongqing, Chongqing 401133, China*
7. *Greater Bay Area Institute for Innovation, Hunan University, Guangzhou 511300, Guangdong Province, China*

Correspondence: maeygzhou@ust.hk (Y. Z), qzz@zzu.edu.cn (Z. Q), gzqin@hnu.edu.cn (G. Q);

Structural Properties

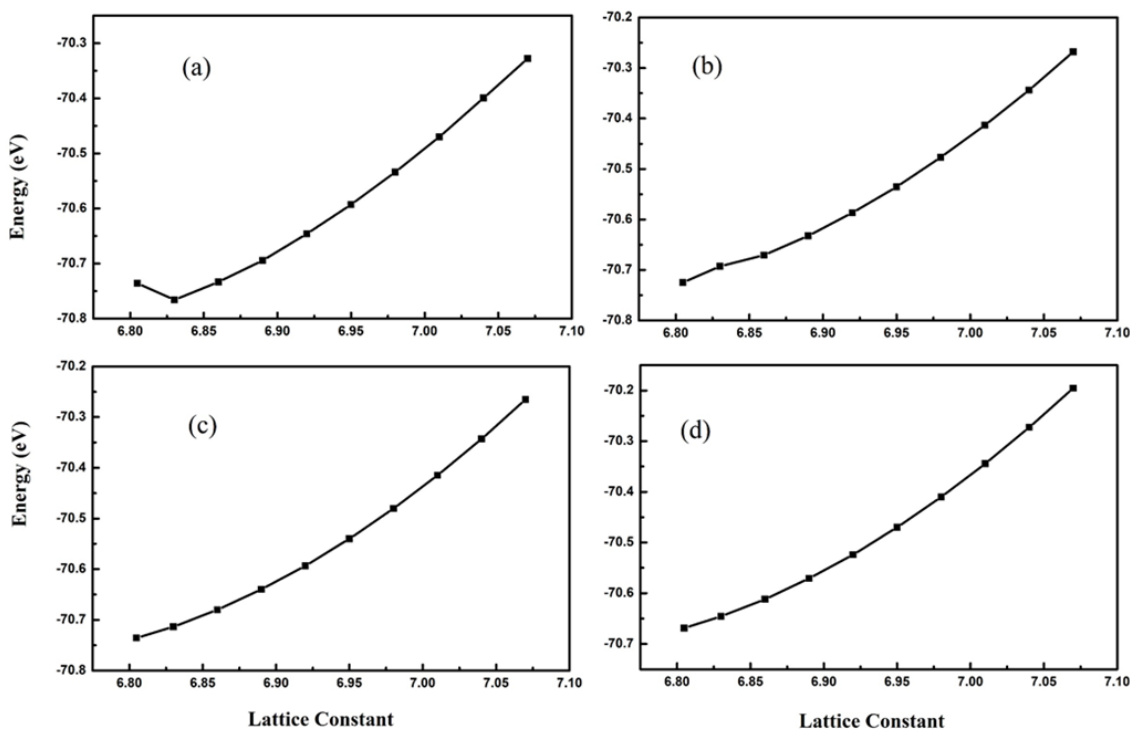


Figure ESI-1: Lattice constants Vs Energy curves for (a) same (b) different interface atoms of AB for (c) same and (d) different interface atoms of AA in $\text{CrI}_3/\text{Br}_3\text{Cr}_2\text{I}_3$ heterostructure.

Figure ESI 1 shows the lattice vs energy curve for exploring the energetically stable lattice constant in each stacking for both the same and different interface atoms. After calculating the stable lattice constant, we further continue our calculations for physical, electronic, and magnetic properties of the heterostructure.

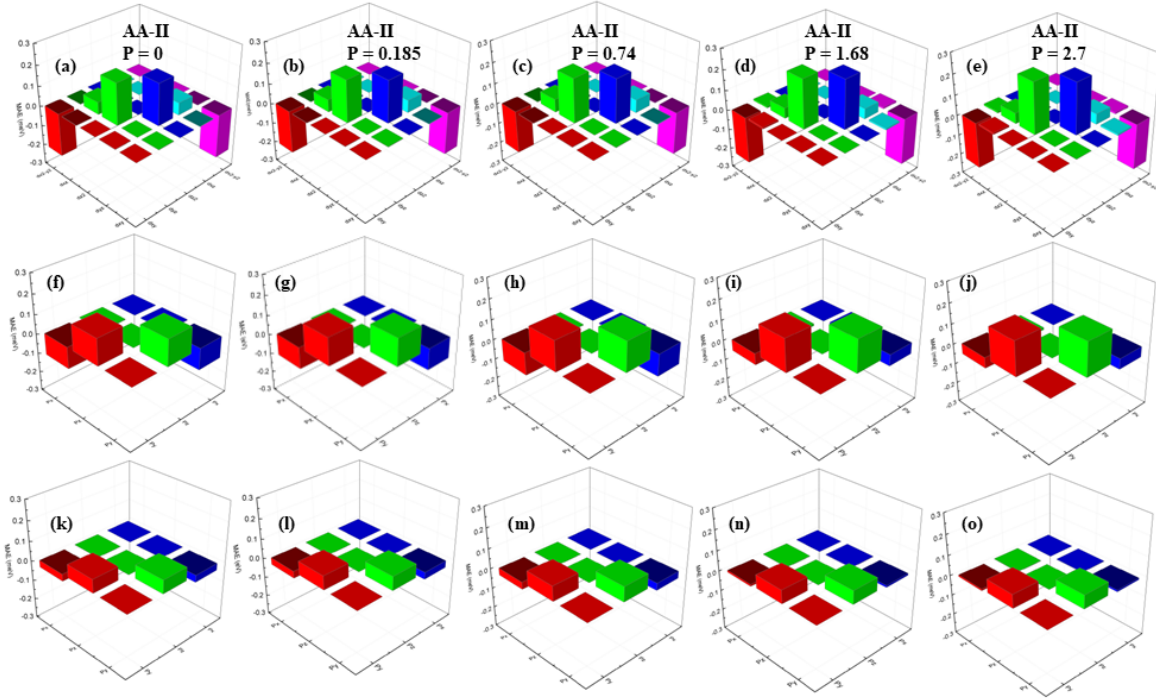


Figure ESI-2: SOC resolved MAE for different interface AA stacking of $\text{CrI}_3/\text{Cr}_2\text{I}_3\text{Br}_3$ heterostructure (a)-(e) for Cr atom, (f)-(j) for I atom and (k)-(o) for Br atoms from zero to 2.7 GPa pressure respectively.

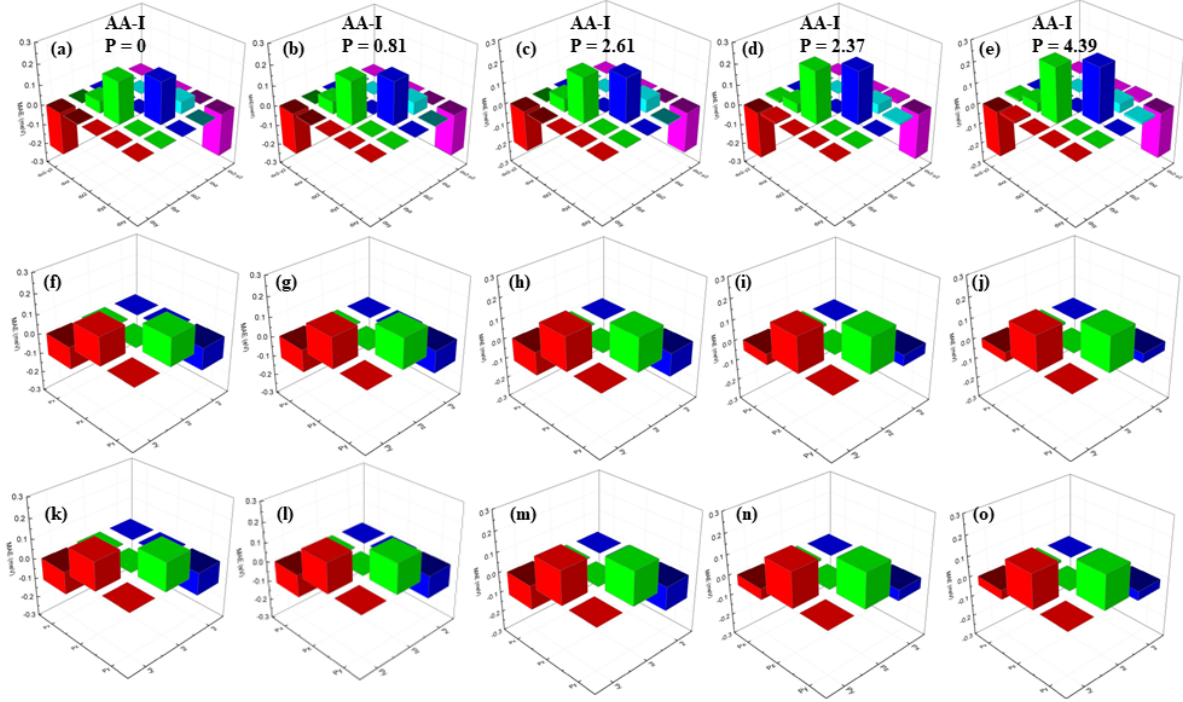


Figure ESI 3: SOC resolved MAE for same interface AB stacking (AA-I) of $\text{CrI}_3/\text{Cr}_2\text{I}_3\text{Br}_3$ heterostructure (a)-(e) for Cr atom, (f)-(o) for I atom from zero to 4.39 GPa pressure respectively.

Figure ESI 2 shows the atomic orbital contributions belonging to both layers (CrI_3 and Janus $\text{Br}_3\text{Cr}_2\text{I}_3$) in the form of $\text{CrI}_3/\text{Br}_3\text{Cr}_2\text{I}_3$ heterostructure. Interestingly, we found an equal contribution from the interface I atom as expected. We also explore the orbital contributions to the MAE for AA stacking in $\text{CrI}_3/\text{Br}_3\text{Cr}_2\text{I}_3$ heterostructure as shown in Figure ESI-3. Hence, the large/small contribution from the interface atoms in either stacking produces large/small values for the MAE. Thus, we get large value of MAE for same interface contact atoms while small value for different irrespective of the stacking. Therefore, we conclude that an increase in atomic size causes an increase in the MAE and vice versa.

We also calculated the charge transfer for AA stacking as given in Table ESI-1 below. We found a similar behavior for the charge transfer in AA stacking. Obviously, we only calculated the amount of charge transfer for the encircled atoms of Figure 1 of the main manuscript. Besides, in the case of AB-I or AA-I, we also consider the Br atom of the surface layer. Furthermore, we found that the charge transfer is more prominent in the Br atoms in the different interface configurations than the same interface configurations. Hence this Bader charge analysis further confirms our charge density difference as given in the main manuscript.

Table ESI-1: Charge transfer (ΔQ) of $\text{CrI}_3/\text{Cr}_2\text{I}_3\text{Br}_3$ heterostructure AB and AA stacking for both same and different contact interfaces. ΔQ measured in e.

	<i>AB</i>		<i>AA</i>	
	I	II	I	II
Cr	-0.14	-0.133	-0.14	-1.14
Br	+0.198	+0.258	+0.194	+0.275
I (Upper)	-0.102	---	-0.104	---
I (Lower)	-0.067	-0.063	0.066	0.067

ΔQ^a the positive and negative signs show the charge accumulation and depletion.

In the following Table ESI-1 and Table-ESI-2, we give the calculated values of Exchange coupling interaction and the Curie temperature at the point of phase transition respectively for AB and AA stacking in $\text{CrI}_3/\text{Br}_3\text{Cr}_2\text{I}_3$ heterostructure. We found that the magnetic moment remains constant irrespective of the stacking and contact configuration.

Table ESI-2: Magnetic moment (μ_B), Third nearest neighbor magnetic exchange coupling energy (J_3) and Curie temperature (T_C) for the AB stacking $\text{CrI}_3/\text{Cr}_2\text{I}_3\text{Br}_3$ heterostructure. μ_B , J and T_C are respectively measured in μ_B , j and K.

	<i>AB-I</i>			<i>AB-II</i>		
	Magnetic moment (μ_B)	J_3 ($\times 10^{-23}$)	T_C (K)	Magnetic moment (μ_B)	J_3 ($\times 10^{-23}$)	T_C (K)
Pristine	3	-0.887	--	3	-1.17	--
5p	3	-0.607	--	3	-0.567	--
10p	3	0.573	95	3	0.789	96
15p	3	2.48	--	3	3.06	--
20p	3	5.74	--	3	6.32	--

Table ESI-3: Magnetic moment (μ_B), Third nearest neighbor magnetic exchange coupling energy (J_3) and Curie temperature (T_C) for the AA stacking $\text{CrI}_3/\text{Cr}_2\text{I}_3\text{Br}_3$ heterostructure. μ_B , J and T_C are respectively measured in μ_B , J and K.

	<i>AA-I</i>			<i>AA-II</i>		
	Magnetic moment (μ_B)	J_3 ($\times 10^{-23}$)	T_C (K)	Magnetic moment (μ_B)	J_3 ($\times 10^{-23}$)	T_C (K)
Pristine	3	-1.63	--	3	-1.64	--
5p	3	-1.45	--	3	-1.45	--
10p	3	-0.628	--	3	-0.599	--
15p	3	1.09	95	3	1.65	95
20p	3	3.82	--	3	4.89	--